

# Chapter 1

## Magnetism

The phenomena of magnetism, like the attraction between pieces of magnetite ( $\text{Fe}_3\text{O}_4$ ) and iron, are well known to mankind since millennia. During all times, magnetism was exploited in groundbreaking technological applications, like e.g. the compass millennia ago<sup>1</sup> and electric power generators in the beginning of the last century. The most recent technological innovation leading to fundamental economic and cultural changes was the development of information technology. In the last two decades, the applied interest in magnetism was mainly due to its application to storage devices and motion sensors.

The phenomenon of magnetism is also of high interest from a scientific point of view. The first successful quantitative description of magnetism was given by classical electrodynamics as presented by James C. Maxwell in 1873 [1] based on the field concept. However, in a microscopic picture, it turned out that magnetism is a very complicated but also fascinating many-particle quantum mechanical phenomenon, which is still not fully understood. It is this combination of high scientific and technological relevance that led to intense research in the last decades. As a result, a rich variety of discoveries were made like the x-ray magnetic dichroism [2–5], interlayer exchange coupling [6] or the giant magneto resistance effect [7, 8] as well as the development of new experimental techniques, e.g. spin polarized scanning tunneling microscopy [9, 10] and resonant magnetic soft x-ray scattering [11]. The following pages introduce the physical concepts related to magnetism of matter that are of relevance in the present work.

### 1.1 Basic Concepts

Matter in the presence of an external magnetic field shows a macroscopic magnetization  $M$  that enhances the external field<sup>2</sup>. Thermodynamically,  $M$  can be expressed as the derivative

$$M(H) = -\frac{1}{V} \left( \frac{\partial F}{\partial H} \right)_T \quad (1.1)$$

of the magnetic Helmholtz free energy  $F$  of a system of volume  $V$  with respect to the magnetic field  $H$  [12]. The quantity describing the response of the material on a field  $H$ , i.e. the amount of change of the magnetization caused by the variation of  $H$ , is the magnetic susceptibility  $\chi$ :

$$\chi = \left( \frac{\partial M}{\partial H} \right)_T \quad (1.2)$$

---

<sup>1</sup>in Europe for about 800 years.

<sup>2</sup>The comparably weak diamagnetic contribution is of no relevance in the present work and is therefore neglected throughout this thesis.

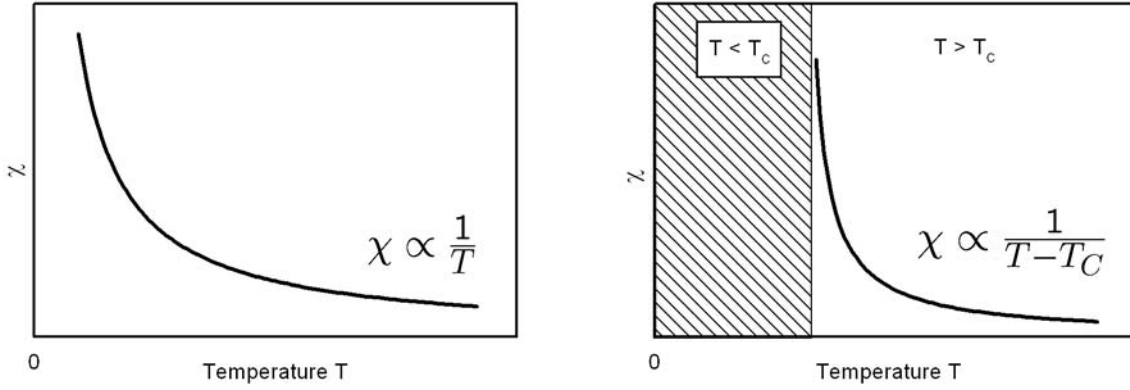


**Figure 1.1:** Temperature dependence of the magnetic susceptibility  $\chi$  of (a) Paramagnets and (b) Ferromagnets.

This behavior originates on a microscopic level from the presence of magnetic moments due to the uncompensated orbital and spin moments of only partly filled atomic shells. These moments tend to align parallel to the external field. Without any interaction between these moments and in the absence of an external field, the mean value of the local magnetization at each place would be zero for all finite temperatures. This behavior is called paramagnetism. In this case, the temperature dependence of  $\chi$  is given by Curie's Law (see Fig. 1.1):

$$\chi \propto \frac{1}{T} . \quad (1.3)$$

A few substances exhibit a non-zero macroscopic magnetization below a material-dependent temperature  $T_C$ , even without an applied field. In this case, the material is called magnetically ordered, with  $T_C$  denoting the ordering temperature. This is caused by an interaction between the microscopic moments, which arises from the minimization of the electrostatic repulsion (Coulomb energy) taking the quantum-mechanical Pauli principle into account: In the simple case of overlapping electronic wave functions, the symmetry of the spatial wave function and consequently the total energy of the system, depends on the spin configuration (Pauli principle), which leads to energetically preferred spin arrangements. This mechanism is called exchange interaction. In the simplest case of only two interacting spins, it is described by the Hamiltonian:

$$H^{spin} = -2JS_1S_2 , \quad (1.4)$$

with  $J$  being the exchange integral that follows from the overlap of the corresponding wave functions.  $J > 0$  favors parallel alignment of the spins,  $J < 0$  antiparallel orientation. A direct overlap of the wave functions is not necessary. On the contrary, the wave functions of the electrons, responsible for the magnetic properties, do not significantly overlap in many interesting magnetic materials, like the transition-metal oxides (e.g. MnO), the lanthanide oxides (e.g. EuO) as well as in the lanthanide metals. In these materials, the exchange is mediated indirectly by other mechanisms, like the famous RKKY interaction (Rudermann and Kittel [13], Kasuya [14], Yosida [15]) that induces the interlayer exchange coupling and the magnetism of the lanthanide metals. In the latter case, the magnetic properties originate from strongly localized  $4f$  electrons, characterized by a negligible inter-atomic overlap, which does not allow a direct exchange between neighboring atoms. Instead, the  $4f - 4f$  coupling between different lattice sites is mediated by the conduction electrons, polarized by intra-atomic exchange with the  $4f$ , which is described in more detail below. The superexchange interaction that

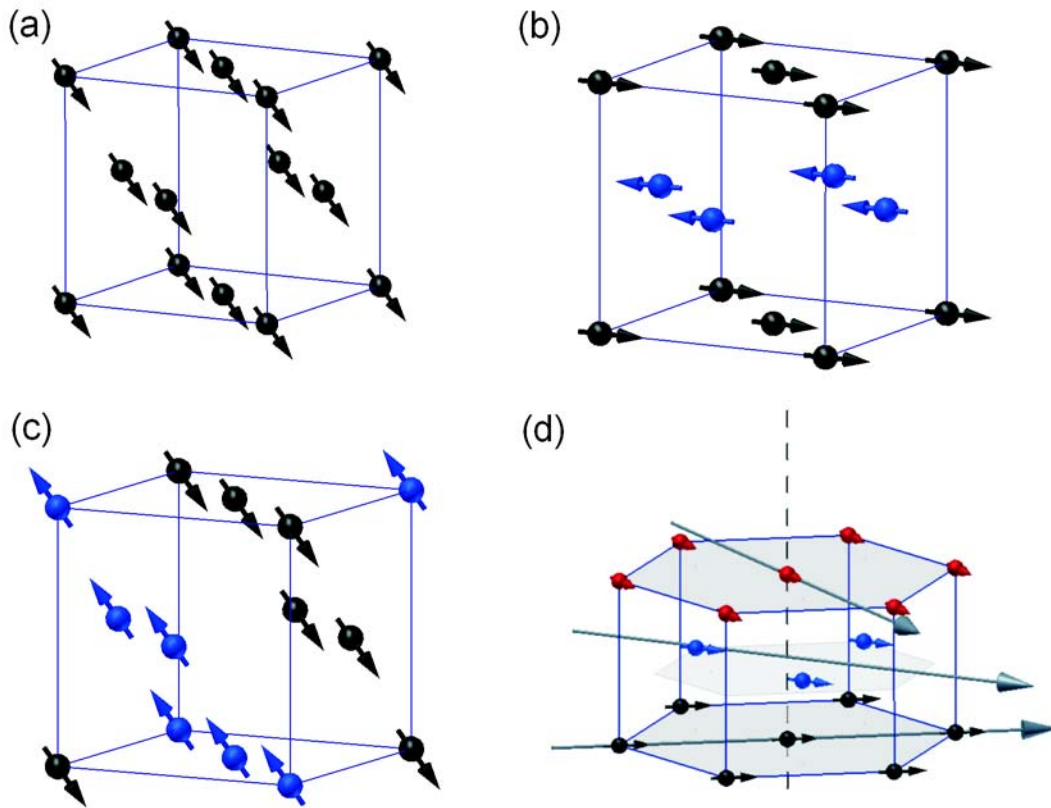


**Figure 1.2:** Some possible magnetic structures of fcc lattices (a-c) and in a hexagonal lattice (d) arising from different exchange mechanisms. The chemical unit cells are shown. The colors indicate the different spin orientations. (a) FM structure as in  $\text{EuO}$  caused by dominant FM nearest-neighbor (nn) interaction (b) AFM type I structure of  $\text{UO}_2$ . (c) AFM type II structure of  $\text{EuTe}$  as a consequence of FM nn and dominant AFM next-nearest-neighbor (nnn) interaction (d) Helical AFM structure of holmium metal due to RKKY exchange interaction. The turning angle of the magnetizations of adjacent ferromagnetically ordered planes of about  $35^\circ$  leads to a long-period AFM modulation with a period of about five hexagonal chemical unit cells along the  $[0001]$  direction.

mediates a coupling via non-magnetic ions represents, in some sense, the counterpart of the RKKY interaction for insulators [16].

In a crystalline solid, the presence of one or several of these coupling mechanisms results in a rich variety of magnetic structures as shown in Fig. 1.2. One can distinguish between magnetic structures showing a non-zero macroscopic magnetization, so called ferri- or ferromagnetic (FM) materials with the ordering temperature named the Curie temperature  $T_C$ , and antiferromagnetic (AFM) structures, where the ordered local moments add to zero. In the latter case, the ordering temperature  $T_N$  is called Néel temperature. Such antiferromagnets usually can be described as to be composed of at least two ferromagnetic sublattices of different magnetization directions [12, p. 695]. The magnetism of all materials studied within this thesis, is caused by strongly localized magnetic moments. Such magnetic structures that consist of spins<sup>3</sup>  $\mathbf{S}_i$ , localized at the ionic positions  $\mathbf{r}_i$ , can be modeled by the

<sup>3</sup>We will neglect the fact that the total magnetic moments usually are not pure spin moments and call the magnetic moments in the following always spin.

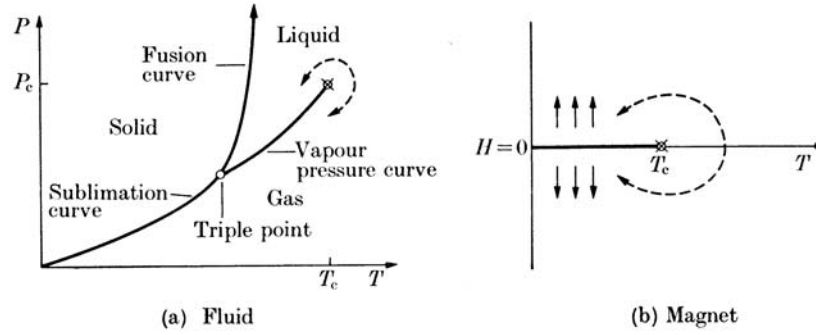


**Figure 1.3:** Phase diagram of (a) water and (b) magnets. The first order phase transition lines are terminated by critical points (from Ref. [18]).

Heisenberg Hamiltonian<sup>4</sup>:

$$H = -\frac{1}{2} \sum_{i,j} J_{|\mathbf{r}_i - \mathbf{r}_j|} \mathbf{S}_i \mathbf{S}_j - g\mu_B H \sum_k (\mathbf{S}_k)_z \quad (1.5)$$

At  $T = 0$  K, the energetic ground state of an ideal Heisenberg ferromagnet, composed of  $N$  spins, is characterized by the parallel alignment of all spins. Hence,  $M$  is equal to the saturation magnetization  $M_{sat} = M(T = 0 \text{ K}) = g\mu_B N S$ . At finite temperatures ( $T > 0$  K), the perfect order is disturbed by thermal disorder. The low-energy elementary excitations are not spin flips (Stoner excitations) but collective modes, called spin waves. Close to  $T = 0$  K, the deviation of the magnetization from the saturation value is given by the  $T^{\frac{3}{2}}$ -law of Bloch [17]:

$$\frac{M(T)}{M(0)} = \left(1 - \left(\frac{T}{\Theta}\right)^{\frac{3}{2}}\right) \quad (1.6)$$

At  $T = T_C$ , the disturbing thermal energy equals the energy gain due to ordering, and the order breaks down. Above  $T = T_C$ , the material then behaves like a paramagnet. This crossover from the paramagnetic to the FM state is called a phase transition.

## 1.2 Phase Transitions

A phase transition is the change of a thermodynamic system from one phase to another. It is characterized by abrupt changes in thermodynamic properties as a consequence of only small variations of a thermodynamical parameter, like the temperature  $T$ . Usually, the two phases differ in their degrees of order and symmetry. Phase transitions can be divided into two categories: First-order transitions are characterized by latent heat and consequently by the coexistence of phases. Examples are the Bose-Einstein condensation, but also familiar effects like the solid-to-liquid, solid-to-gas, and liquid-to-gas transitions, while crossing the fusion, sublimation, and vapor-pressure curves, respectively, as shown in Fig. 1.3. The vapor-pressure curve is terminated at the critical point. Therefore, it is possible to convert a liquid to a gas continuously, without crossing a phase transition line. At the critical point, the liquid-to-gas transition exhibits no latent heat and no phase mixing. This is a characteristic of a continuous or second-order phase transition. Other examples for continuous phase transitions are

<sup>4</sup>H defines the z direction.

quantity	exponent	power law	$t$
specific heat	$\alpha$	$C_V \propto t^{-\alpha}$	$> 0$
magnetization	$\beta$	$M \propto (-t)^\beta$	$< 0$
susceptibility	$\gamma$	$\chi \propto t^{-\gamma}$	$> 0$
correlation length	$\nu$	$\xi \propto t^{-\nu}$	$> 0$
pair correlation function	$\eta$	$G(\mathbf{r}) \propto  \mathbf{r} ^{-(d-2+\eta)}$	$0$

**Table 1.1:** Critical exponents describing the ferromagnetic phase transition close the critical point ( $T = T_C$ ,  $h = 0$ ) [18]. The parameter  $d$  denotes the dimensionality of the system.

the superfluid transition and the ferro/paramagnetic transition. Since such continuous transitions are associated with critical points, the associated phenomena are called critical phenomena. They are characterized by singularities in many thermodynamic quantities at the critical point as shown for the susceptibility in Fig. 1.1. Close to the critical point, these quantities can be described by power laws [18, chapter 3.1]:

$$f(t) \propto t^{-\lambda} \quad , \quad (1.7)$$

with  $f$  a thermodynamic quantity and

$$\lambda = \lim_{t \rightarrow 0} \frac{\ln f(t)}{\ln t} \quad , \quad (1.8)$$

the critical exponent. The dimensionless reduced temperature  $t$ ,

$$t = \frac{T - T_C}{T_C} \quad , \quad (1.9)$$

quantifies the difference in temperature from the critical point. Each quantity having a critical exponent less than zero diverges at  $T_C$ , or becomes zero otherwise. Table 1.1 summarizes power-law behaviors predicted for magnetic phase transitions.

The classical theories of ferromagnetism<sup>5</sup> and phase transitions<sup>6</sup> can successfully describe the general magnetic behavior, in particular at low temperatures. However, all of them fail to determine quantitatively correct values for the critical exponents, predicting, for example,  $\beta = 0.5$  to be independent of the material [19, chapter 7.2], in striking contrast, e.g., to the experimental finding of  $\beta = 0.335$  by Heller and Benedek on AFM  $\text{MnF}_2$  [20]. This breakdown of the classical theories led to phenomenological descriptions based on the concept of scaling invariance [21, 22]. Their predictions could be derived from first principles within the renormalization group (RG) theory by Wilson and others [23–26]. The results are precise predictions for the values of the critical exponents as well as a set of four scaling relations connecting the six critical exponents<sup>7</sup> [19]:

$$\begin{aligned} \alpha + 2\beta + \gamma &= 2 \\ (2 - \eta)\nu &= \gamma \\ \alpha + \beta(\delta + 1) &= 2 \\ 2 - \alpha &= d\nu \quad . \end{aligned}$$

<sup>5</sup>e.g. Molecular field theory of Weiss.

<sup>6</sup>e.g. Landau's theory.

<sup>7</sup>In addition to the five exponents given in table 1.1, the critical exponent  $\delta$  describes the dependence of the magnetization on a field  $h$  in the limit  $h \rightarrow 0$ .

model	$\beta$	$\gamma$	$\nu$
2D Ising [19]	0.1250	1.750	1.000
3D Ising [33]	0.3250	1.240	0.630
3D XY [33]	0.3460	1.316	0.669
3D Heisenberg [33]	0.365	1.387	0.705
mean-field theory [19]	0.5	1	0.5

**Table 1.2:** Critical exponents derived within various theoretical models.

Thus, the whole set of exponents is known as soon as two of them are determined. Many experiments were performed concerning bulk critical behavior [27–32] and the experimental results completely confirm these theoretical predictions.

The quantitative description of a phase transition is based on the definition of an order parameter, like the magnetization for magnetic phase transitions, which measures the degree of long-range order. Its thermal average is zero in one phase, but non-zero in the other one, vanishing continuously towards the critical point. It is a remarkable fact, that the order parameters of different systems show a very similar critical behavior. Independent of the microscopic origin of the long-range order, the critical behavior seems to be insensitive to the microscopic details. It depends on the dimensionalities of the system  $d$  and the order parameter  $D$ , only. This phenomenon is called universality [19, ch. 1.4]. Therefore, each experimental study of the critical behavior of an individual sample provides knowledge on a much larger class of systems. Table 1.2 gives the critical exponents predicted for the most prominent models applied to magnetic phase transitions. The reason for the universal critical behavior is the occurrence of fluctuations in the order parameter that cover all length scales at  $T = T_C$ . Therefore, the key value in the description of the critical phenomena is the extension of these fluctuations, i.e. the size of the regions of correlated spins, which is quantified by the correlation length  $\xi$ . The fluctuations can be described by the two-point correlation function [19]:

$$G(\mathbf{r}_i, \mathbf{r}_j) \equiv \langle \mathbf{m}_i \cdot \mathbf{m}_j \rangle \quad , \quad (1.10)$$

where  $\mathbf{m}_i = \mathbf{m}(\mathbf{r}_i)$  denotes the local magnetization at the position  $\mathbf{r}_i$ . In isotropic systems,  $G$  only depends on the distance  $r = |\mathbf{r}_i - \mathbf{r}_j|$  and can be written as:

$$G(r) \equiv G_c(r) + |\langle \mathbf{M} \rangle|^2 \quad , \quad (1.11)$$

with

$$G_c(r) \equiv \langle \mathbf{m}(0) \cdot \mathbf{m}(r) \rangle - |\langle \mathbf{M} \rangle|^2 \quad . \quad (1.12)$$

While the long-range order contributes to the correlation function  $G$ , the connected two-point correlation function  $G_c$  exclusively probes the fluctuations. Figure 1.4 clarifies the different contributions. Well below the ordering temperature,  $G_c(r)$  is small, and the long-range order represents the dominant contribution to the correlation function. Above  $T_C$ , the long-range order has vanished, and  $G_c(r)$  is the only remaining contribution. Above  $T_C$ ,  $G(r)$  is approximately described according to the Ornstein-Zernike approximation for large  $r$  by [18, p. 105]:

$$G(r) \propto \frac{e^{-\frac{r}{\xi}}}{r} \quad . \quad (1.13)$$

The correlation functions can be accessed by several experimental techniques. SQUID and MOKE, e.g. , measure the average magnetization  $\langle M \rangle$ , while ac-susceptibility measurements probe  $G_c(r)$

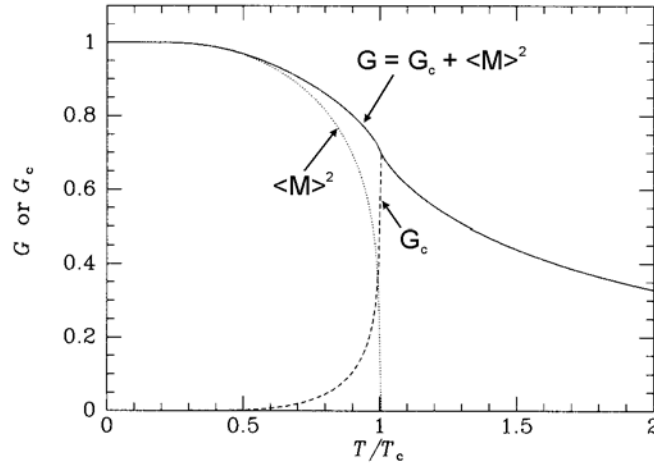


**Figure 1.4:** Different contributions to the two-point correlation function (after Ref. [19]).

[34]. Magnetic scattering techniques are sensitive to  $G(r)$ , which provides access to  $\langle M \rangle$  below  $T_C$  as well as to the critical fluctuations above the ordering temperature. Therefore, magnetic scattering experiments can quantify a number of critical exponents, e.g.  $\beta$ ,  $\nu$ ,  $\gamma$  and  $\eta$ , independently. Note, this enables, on the one hand, to test the validity of the scaling relations, but otherwise allows to determine the entire set of critical exponents of the studied phase transition. It is for this reason, that most of the experimental tests of the scaling relations exploited scattering techniques.

The critical behavior is a consequence of the divergence of  $\xi$  at the critical point, which is only possible in a perfect, infinite system. Therefore, the behavior of a real and hence finite system will differ from the situation discussed so far.

A simple theoretical example is illustrated in Fig. 1.5, which shows the specific heat  $C$  of a two-dimensional  $n \times n$  Ising lattice with periodic boundary conditions. While the divergence of  $C$  to infinity is suppressed in the finite lattice, it still shows a pronounced maximum of increasing height with increasing system size, deviating from the behavior of the ideal infinite system in a range around the critical point, which becomes rather large only in the limit of small  $n$ . Since the finiteness of real systems is accompanied by a surface, our knowledge of magnetism is incomplete as long as we neglect finite-size effects and the influence of a surface on the magnetism of a material. Such effects are in particular interesting from a technological point of view as a consequence of sustained miniaturization tendency in information technology and the importance of interface properties in current and future applications.

### 1.3 Surface and Finite-Size Effects

From a theoretical point of view, one can distinguish between pure finite-size effects and altered behavior due to the presence of a surface. The main consequences of finiteness are a rounding of the divergences of the macroscopic thermodynamic quantities and a shift of the temperature of the maxima as shown in Fig. 1.5. A surface, on the other hand, introduces local variations of the thermodynamic quantities at the boundary as a result of the broken symmetry, even in a semi-infinite system. From an experimental point of view, this differentiation is only partly applicable, since real finite systems usually have a surface. Therefore, the following discussion distinguishes between macroscopic

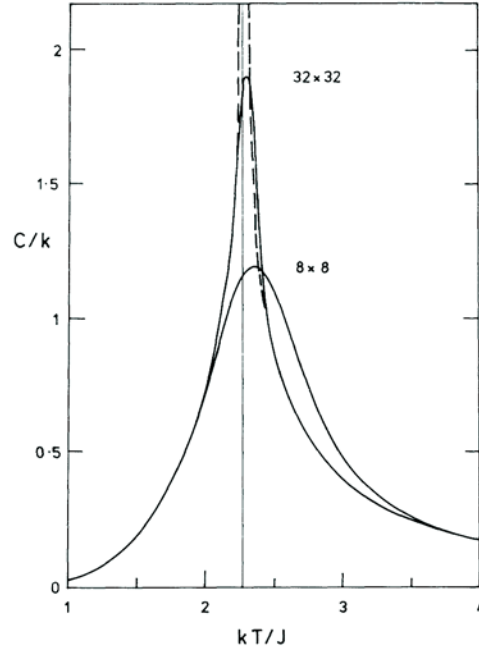


**Figure 1.5:** Influence of size on the specific heat of an  $n \times n$  square Ising lattice with periodic boundary conditions after Ferdinand and Fisher for  $n = 8$  and  $n = 32$ . The dashed line corresponds to the specific heat of an infinite lattice (from Ref. [35]).

and local effects. An altered macroscopic behavior, for example a change of the ordering temperature, typically is restricted to samples with at least one strongly limited spatial dimension, which is the subject of the following section.

### 1.3.1 Reduced Ordering Temperature and Dimensional Crossover

Any macroscopic quantity can be divided into a bulk part and a surface part [36]. The relative contribution of the surface is given by the ratio of the number of bulk spins and the number of spins influenced by the surface. The influence of the surface is limited to a layer of thickness  $\xi$ . Considering a cubic system of size  $L^3$ , the relative contribution of the surface is of the order of  $\frac{\xi L^2}{L^3} = \frac{\xi}{L}$ . Thus, as long as  $\xi \ll L$ , the effect of the surface on a macroscopic quantity is negligible. However, in nano-structured systems, like thin films, dots or lines, the presence of the surface represents a severe perturbation. In such systems, changes in the temperature-dependent behavior occur, once the diverging correlation length becomes comparable to the spatial dimension of the sample. A well-known example is the decreasing ordering temperature with decreasing sample thickness. This effect was observed for thin films of the 3d-magnets Fe [37], Co [38], Ni [39], and for thin FM films of the lanthanide metal gadolinium [40], but also for the simple antiferromagnet CoO [41]. In a molecular field picture, this so-called finite-size effect on the ordering temperature is caused by the increasing relative amount of surface spins. The lack of neighbors at the surface leads to a reduced mean exchange energy, which lowers the ordering temperature. The observed thickness dependence,  $T_C(d)$ , is described in all of the above-mentioned studies by the theoretically predicted scaling relation [42, 43]:

$$\frac{T_C(\infty) - T_C(d)}{T_C(\infty)} = bd^{-\lambda} \quad , \quad (1.14)$$

with the shift exponent  $\lambda$  given by

$$\lambda = \frac{1}{\nu} , \quad (1.15)$$

and  $\nu$  being the critical exponent of the bulk correlation length. The same behavior was found for the lateral limitation in Fe stripes [44]. On the other hand, a modified shift of the ordering temperature

$$\frac{T_C(\infty) - T_C(d)}{T_C(d)} = b'(d - d_0)^{-\lambda'} , \quad (1.16)$$

including an offset thickness  $d_0 = 42 \text{ \AA}$ , was observed for Cr in Cr/Fe multilayers [45]. This finding was related to a long-period incommensurate spin-density wave in combination with spin-frustration due to the exchange coupling with the FM iron at the rough interfaces. However, a recent study on single films of the long-period helical antiferromagnet holmium revealed essentially the same modified thickness dependence, but with  $d_0 \approx 10$  monolayers (ML) [46]. The offset values  $d_0$ , found for the two materials, match the period lengths of the studied AFM structures, suggesting that this modification in the behavior of long-period antiferromagnets is more fundamental.

The ordering temperature is commonly identified by the anomalies of  $\chi$ ,  $\xi$  or  $C$ . The corresponding critical exponents yield information on the universality class of the phase transition. In thin films, the divergence of the correlation length is limited by the thickness of the sample, which causes a change of the critical behavior towards rather two-dimensional behavior. This so-called dimensional crossover, was indeed observed as a function of film thickness in several experiments on thin films of Fe, Co and Ni [39, 47–49] as well as on Gd [50]. The dimensional crossover was identified by characteristic changes of the critical exponents. Most of the studies focused on the value of  $\beta$ , obtained from temperature-dependent measurements of the macroscopic magnetization. Even in thicker samples, the behavior should be 2D-like in the vicinity of the ordering temperature, once the divergence of the correlation length is truncated by the finite sample thickness. According to RG-theory, the divergence of the correlation length normal to the surface of a thin film is truncated at about one third of the film thickness  $L$ , i.e.  $\xi < \frac{L}{2.89}$  [51, 52]. This theoretical prediction was confirmed for the first time by Nickel et al. in a study of the structural order-disorder transition of thin FeCo-films [53]. A recent experiment on thin holmium films revealed a comparable crossover as a function of film thickness and temperature [54], concluded from distinct changes of the temperature dependence of the correlation length.

In all mentioned studies, the modifications of the macroscopic properties due to spatial limitations are restricted to ultra-thin films or to a very narrow temperature regime in the vicinity of the ordering temperature. This does not hold for local properties as discussed in the following.

### 1.3.2 Magnetization Profiles

The most obvious consequence of a surface is the loss of translational invariance and isotropy, which leads to a reduced coordination number for the surface spins. Therefore, one could expect that these surface spins are less tightly embedded into the ordered magnetic structure and consequently the magnetization of the surface layer to be reduced with respect to the bulk value. This is indeed predicted by theory.

Close to  $T = 0 \text{ K}$ , the spin-wave theory of finite systems [55] predicts the deviation from the saturation magnetization at the surface to be twice as large as in the bulk. In 1974, Kurt Binder and Pierre Hohenberg published [56] their pioneering Monte-Carlo (MC) study of the temperature dependence of the surface magnetization in finite Ising and Heisenberg magnets. They showed that in the entire temperature range of the ordered phase ( $t < 0$ ), such systems exhibit a distinct magnetization profile

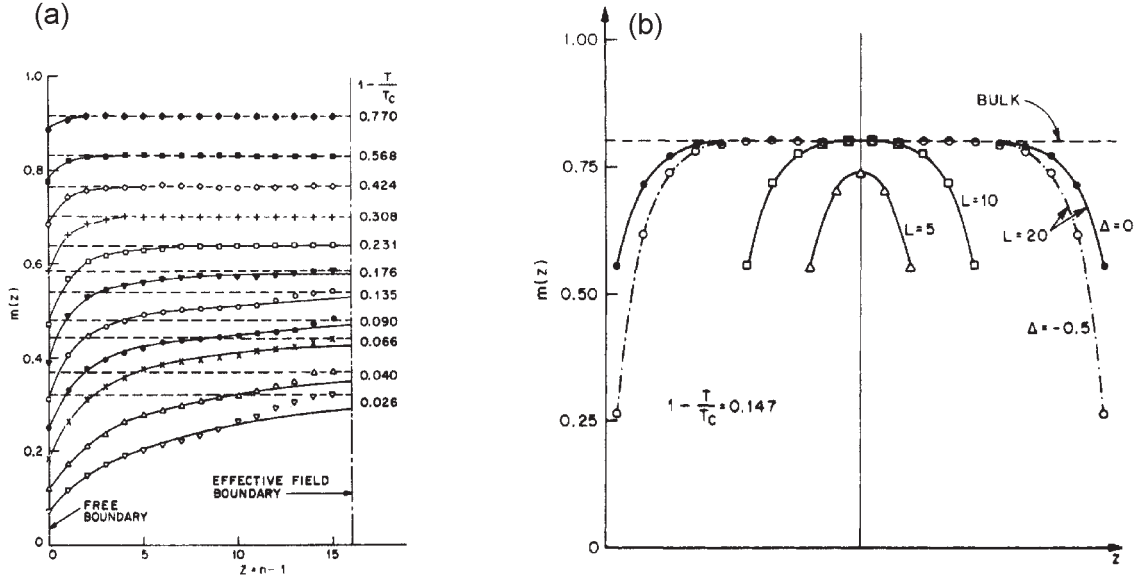


**Figure 1.6:** Magnetization profiles at finite temperatures obtained by means of Monte-Carlo simulations by Binder and Hohenberg of (a) a semi-infinite FM Heisenberg system and (b) a FM Ising system with two free surfaces and periodic boundary conditions at the remaining four sides at  $t = -0.147$  (from Ref. [56]).

along the surface normal with a reduced magnetization at the surface as displayed in Fig. 1.6. Obviously, such magnetization profiles are a general feature of magnetic surfaces as evident from their occurrence in the Heisenberg as well as in the Ising case. Despite the very similar overall behavior of the Heisenberg and the Ising lattices, the two systems differ in the details of the evolution with temperature. The magnetization profile of the Ising lattice is characterized by a fast exponential decay of the deviation of the magnetization from the bulk value, from the surface towards the center of the film. Consequently, the number of layers affected by the surface is rather small well below  $T_C$  ( $< 5$  ML). That does not hold for the Heisenberg systems. Over a large range of temperature, the deviation of the magnetization  $m(z)$ , at distance  $z$  from the surface, from the bulk value  $m_b$  is described by a power law:

$$m_b - m(z) \propto \frac{\xi}{z}, \quad (1.17)$$

in excellent agreement with the predictions of the spin-wave theory. Even close to the ordering temperature, they found the characteristic  $z^{-1}$  dependence in the limit of large  $z$ . The critical behavior, on the other hand, was found to be rather undisturbed by the presence of spin waves. These results of Binder and Hohenberg suggest that normal to the surface of a magnet a pronounced magnetization profile can be found at each finite temperature ( $t < 0$ ), independent of the universality class of the corresponding infinite system.

However, the situation at the surface can be more complicated in real systems. Changes of the electronic structure close to the surface or surface reconstruction can alter the coupling strength at the surface  $J_S$ . This different spin interaction at the surface can be quantified by the so-called surface

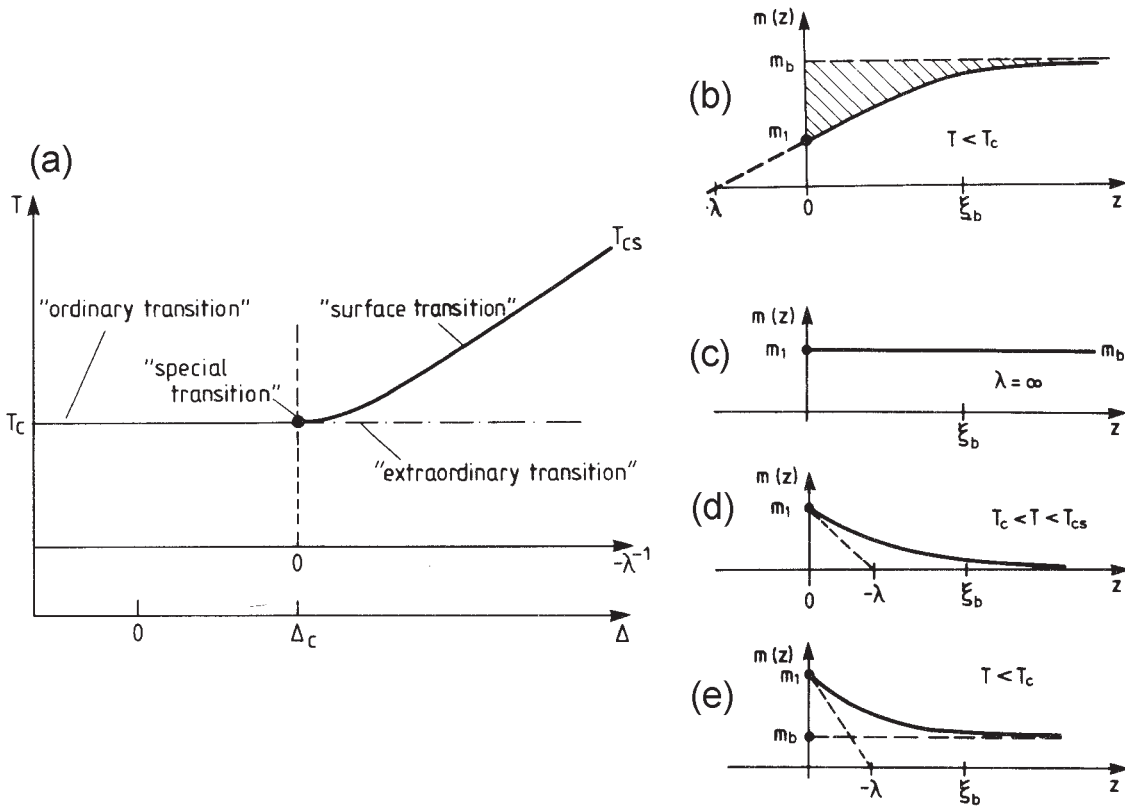


**Figure 1.7:** Phase transitions at the surface layer of a semi-infinite magnetic system. (a) Phase diagram. The phase transition depends on the surface enhancement  $\Delta$  plotted at the axis of abscissae. The associated schematic magnetization profiles according to Ginzburg-Landau theory: (b) Ordinary transition (c) Special transition (d) Surface transition  $T_C^{surf} > T > T_C^{bulk}$  (e) Extraordinary transition  $T < T_C^{bulk}$  (after Ref. [57]).

enhancement  $\Delta$ :

$$J_S = (1 + \Delta)J_{bulk} \quad . \quad (1.18)$$

The theoretically expected magnetic behavior at the surface strongly depends on  $\Delta$  as seen in the phase diagram in Fig. 1.7(a) [57]. For a rather unchanged coupling strength at the surface ( $\Delta \approx 0$ ), the surface order is predicted to occur at the bulk critical temperature  $T_C^{bulk}$ . The associated transition is called to be of the ordinary type. In this case, the magnetization of the surface layer  $m_1$  is reduced with respect to the bulk value. As a consequence, a magnetization profile is present that links  $m_1$  and  $m_b$  as shown in Fig. 1.7 (b). The number of layers affected from the surface is related to the temperature-dependent correlation length  $\xi$ . Close to the surface ( $z \ll \xi$ ), the profile is predicted to vary as:

$$m(z) \propto z^{\frac{\beta_1 - \beta_b}{\nu}} \quad , \quad (1.19)$$

where  $\beta_b$  and  $\nu$  denote the critical exponents of the bulk magnetization and the correlation length, respectively, and  $\beta_1$  is an additional critical exponent related to the surface layer, which is discussed in detail below. In the other limit ( $z \gg \xi$ ), the deviation of the magnetization from the bulk value

quantity	symbol	exponent
layer magnetization	$m_1$	$\beta_1$
layer susceptibility	$\chi_1$	$\gamma_1$
surface susceptibility	$\chi_{11}$	$\gamma_{11}$
two-point correlation function	$G_{\parallel}$	$\eta_{\parallel}$
two-point correlation function	$G_{\perp}$	$\eta_{\perp}$

**Table 1.3:** *Thermodynamic quantities describing the magnetic surface and associated critical exponents.*

decreases exponentially fast<sup>8</sup> as

$$m_b - m(z) \propto e^{-\frac{z}{\xi}} . \quad (1.20)$$

On the other hand, for a significantly enhanced value of  $\Delta$ , the surface orders at a temperature  $T_C^{surf}$  (surface transition), which is larger than the temperature  $T_C^{bulk}$ , where the bulk order occurs (extraordinary transition). The intermediate temperature regime,  $T_C^{bulk} < T < T_C^{surf}$ , is characterized by the presence of a paramagnetic bulk with the surface already ordered. In this temperature regime, the magnetization decays exponentially fast from its maximum at the surface towards zero in the bulk, with a typical decay length given by the correlation length  $\xi$  as shown in Fig. 1.7(d). Ordinary and extraordinary transitions are separated by the multicritical point,  $(\Delta = \Delta_c, T = T_C^{bulk} = T_C^{surf})$  (special or surface-bulk (SB) transition). Note, it is only this case, characterized by a surface enhancement that precisely counterbalances the influence of the altered coordination number of the surface spins, which is associated with an order parameter without any spatial variation (see Fig. 1.7(c)). An ideal Heisenberg system should neither show the extraordinary nor the special transition for both are related to the ordering of the two-dimensional surface, which was proven not to be possible [58]. However, the presence of an easy-axis surface anisotropy can lead to an Ising-like surface transition [59].

In the following, we will focus on the ordinary transition. The description of the altered surface behavior requires additional local thermodynamic variables, e.g. the magnetization of the first layer  $m_1$  or the layer susceptibility  $\chi_1$ . As in the case of the infinite system, the temperature dependence of the local thermodynamic quantities is described by power laws, with critical exponents that differ from those of the corresponding bulk properties (see table 1.3). The surface critical behavior obeys the principle of universality and does not introduce a second critical length scale [57]. Also close to the surface the temperature dependence of the size of the critical fluctuations is governed by the bulk correlation length  $\xi$ . Like the bulk exponents, the surface exponents are not independent. They are interrelated by additional scaling laws [36, 57], like:

$$\begin{aligned} \beta_1 &= \frac{\nu}{2}(d - 2 + \eta_{\parallel}) \\ \gamma_1 &= \nu(2 - \eta_{\perp}) \\ \gamma_{11} &= \nu(1 - \eta_{\parallel}) \\ \eta_{\perp} &= \frac{\eta + \eta_{\parallel}}{2} . \end{aligned}$$

Therefore, only one additional exponent determines the surface critical behavior [60]. Several theoretical studies (see table 1.4) on the Heisenberg model predict  $\beta_1$  to be about 0.8, which significantly deviates from the bulk value of  $\beta = 0.365$ . It was further shown that  $\beta_1$  is not sensitive to

---

<sup>8</sup>This result holds for the Ising model.

system	$\beta_1$	reference
3D Heisenberg	$0.75 \pm 0.1$	Binder and Hohenberg [56]
3D Heisenberg	$0.834 \pm 0.006$	Krech [62]
FM Ni (100)	$0.825^{+0.025}_{-0.04}$	Alvarado [63]
FM Ni (111)	$0.70 \pm 0.09$	Voigt [64]
FM EuS (111)	$0.72 \pm 0.03$	Dauth [65]
AFM NiO (001)	0.89	Namikawa [66]

**Table 1.4:** Theoretical and experimental results for  $\beta_1$ .

surface bond disorder or steps at the surface [61]. Hence, the determination of  $\beta_1$  became the common method to identify surface critical behavior experimentally.

Numerous experiments confirmed the predicted altered behavior close to the surface by means of extremely surface sensitive or local techniques like Mössbauer spectroscopy, spin-polarized LEED (SPLEED), spin-polarized electron capture, or NMR. In 1979, Celotta et al. [67] observed a rather linear decrease of the magnetization at the surface of a Ni(110) single crystal in striking contrast to the known bulk critical exponent  $\beta = 0.33$ . A later study on the Ni(110) surface [63] quantified  $\beta_1 = 0.825$  and  $T_C^{bulk} = T_C^{surf}$ , in excellent agreement with the theoretical predictions for ordinary behavior. Similar result were found by Dauth [65] for the (111) surface of the prototypical Heisenberg ferromagnet EuS and by Namikawa on AFM NiO(001) [66] on NiO(001). Table 1.4 summarizes the discussed experimental results. From these theoretical and experimental results, it is apparent that, in general, the magnetization is not a constant but exhibits a magnetization profile along the surface normal.

The experimental observation of such magnetization profiles poses a challenge, for most of the methods that measure the magnetization are integrating methods. Thus, only the mean macroscopic magnetization or, in the case of surface sensitive methods, the magnetization of the outermost layer can be measured. To observe the profiles, experimental methods of high-resolution depth sensitivity are required. The studies carried out so far typically were based either on site-sensitive methods like PAC [64, 68] or a combination of techniques of different depth sensitivity [69]. Following the latter approach, Pfandzelter et al. studied the Fe(110) surface combining MOKE, electron emission and electron capture techniques. They found depth-dependent magnetizations, characterized by a reduced value at the surface. Similar results were obtained from the Ni(111) surface by Voigt et al. [64] by means of the perturbed  $\gamma\gamma$  angular correlations method (PAC). The results of these two studies are in good agreement with the theoretical predictions discussed above. However, both methods are characterized by an enormous experimental effort and consequently an atomic-layer-resolved magnetization profile across an entire sample never was reported.

Magnetic scattering techniques, on the other hand, can achieve depth sensitivity, exploiting the strongly varying photon penetration depth across absorption thresholds [70] and in the vicinity of total reflection [60]. But also at larger angles of incidence, the shape of a diffraction pattern can strongly depend on details of the individual-layer magnetizations, and as long as the number of contributing magnetic layers is rather small, a reconstruction of the magnetization profile may be feasible, which is demonstrated in this thesis.

